Article **Journal of Technological Engineering**
December 2023, Vol.7 No.20 1-9

Characterization of a dual system of hydraulic cylinders to originate tilting movement and column support in an industrial furnace

Caracterización de un sistema dual de cilindros hidráulicos para originar movimiento basculante y del soporte en columna en un horno industrial

TÉLLEZ-MARTÍNEZ, Jorge Sergio´*†, SÁNCHEZ-HERNÁNDEZ, Miriam Zulma´, KANTUN-UICAB, María Cristina´´ and PACHECO-SANTAMARÍA, Gerardo´´´

´*Tecnológico Nacional de México / Instituto Tecnológico de Morelia, Morelia 58120, México.*
´´*Universidad Politécnica de Juventino Rosas. Procesos de Manufactura y Materiales Avanzados. Miguel Hidalgo 102, Comunidad de Valencia, Santa Cruz de Juventino Rosas, Gto.; México.*
´´´*Universidad Politécnica de Juventino Rosas. Academia de Ingeniería en Manufactura Avanzada. Miguel Hidalgo 102, Comunidad de Valencia, Santa Cruz de Juventino Rosas, Gto.; México.*

ID 1st Author: *Jorge Sergio, Téllez-Martínez* / **ORC ID:** 0000-0003-0587-0059, **CVU CONAHCYT ID:** 40084

ID 1st Co-author: *Miriam Zulma, Sánchez-Hernández* / **ORC ID:** 0000-0001-6230-6986

ID 2nd Co-author: *María Cristina, Kantun-Uicab* / **ORC ID:** 0000-0003-1588-5414, **CVU CONAHCYT ID:** 162342

ID 3rd Co-author: *Gerardo, Pacheco-Santamaría* / **ORC ID:** 0009-0004-2105-5171, **CVU CONHACYT ID:** 348373

DOI: 10.35429/JTEN.2023.20.7.1.9 Received July 10, 2023; Accepted December 30, 2023

Abstract

The controlled displacement of large masses or response to loads is guaranteed by implementing hydraulic systems. The capacity of these systems implies the cylinders' design and the pump power that drives the working fluids. In this regard, the reference to the construction planning of an industrial melting furnace is an example of analysis. Before determining the characteristics of the implicit hydraulic systems, the required element displacement magnitudes were determined. In addition to the load profiles according to the geometric and density characteristics of the materials used to consolidate the equipment during operating conditions, the data obtained by applying reaction analysis and the concept of force multiplication (Pascal's law) determined the equipment characteristics. Likewise, these characteristics are used to select the commercial elements, considering a safety factor for good performance.

Angle joint design, Hydraulic systems, Assisted displacement

Resumen

El desplazamiento controlado de grandes masas o respuesta a cargas se garantiza con la implementación de sistemas hidráulicos. La capacidad de estos sistemas implica el diseño de los cilindros y de la potencia de la bomba que impulse el fluido de trabajo. Al respecto, la referencia a la planeación de construcción de un horno de fusión industrial se utiliza como un ejemplo de análisis. Previo a la determinación de las características de los sistemas hidráulicos implícitos se determinaron las magnitudes de desplazamiento de elementos requeridas. Además de los perfiles de carga de acuerdo con las características geométricas y de densidad de los materiales utilizados en la consolidación del equipo durante condiciones operativas. Los datos obtenidos aplicando el análisis de reacciones y el concepto de multiplicación de fuerza (Ley de Pascal) se determinaron las características del equipo. Asimismo, estas características se utilizaron para la selección de elementos comerciales considerando un factor de seguridad para un buen desempeño.

Diseño de articulaciones angulares, Sistemas hidráulicos, Desplazamiento asistido

Citation: TÉLLEZ-MARTÍNEZ, Jorge Sergio, SÁNCHEZ-HERNÁNDEZ, Miriam Zulma, KANTUN-UICAB, María Cristina and PACHECO-SANTAMARÍA, Gerardo. Characterization of a dual system of hydraulic cylinders to originate tilting movement and column support in an industrial furnace. Journal of Technological Engineering. 2023. 7-20:1-9.

* Correspondence from the Author (E-mail: jorge.tm@morelia.tecnm.mx)
† Researcher contributing as first author.

Introduction

In the hydraulic loading power systems terminology, piston cylinders are also called skid steer loaders used in various devices. For example, researchers (Dadhania, Bhatiya, Joshi, & Sharma, 2016) conducted a literature review on the design of the tilting mechanism of cabins in loading vehicle. These work vehicles also implement complex displacement systems controlled by hydraulic cylinders. Researchers (Xu & Yoon, 2016) reviewed the kinematic and dynamic modeling of the mechanical link in assisted blade joints and presented several modeling approaches in the hydraulic system. Other analyses of multiple cylinders acting on platforms are sparsely reported (Hu, et al., 2022), (Sun & Chiu, 2001). In the case of commercialized tilting furnaces, it is evident that the design of hydraulic systems is standardized and developed by the companies that manufacture them, (Nabertherm, 2023). However, design engineering information is confidential except in the corresponding patents or some incipient reports at conferences (Audet, Parent, Deveaux, & Courtenay, 2004).

Figure 1 Melting furnace implementing: a) joint for tilting, b) joint for opening the lid
Source: Images property of Mechatronics DDMI COMBUSTION.
https://www.youtube.com/watch?v=LP3Wmo8rSlU

Therefore, through the analysis of the trajectory of joint displacements and a force balance based on reactions, it was proposed to obtain the characteristics of hydraulic cylinders with specific loading conditions for the construction of equipment similar to that shown in Figure 1, and to define the programming bases of a computer application that allows calculating variants. The objective was to obtain an analysis methodology for characterizing hydraulic cylinders acting in pairs in a symmetrical system considering a pseudo-static load. Given the extent of development of this work, a work published simultaneously by the primary author supports the analysis of the geometry of assisted joints implemented for tilting.

Methodology

Reaction analysis consists of making equilibrium diagrams of the system subjected to loads. Addressing the two cases relevant to determining the analysis strategy allows us to understand the objective results. First, the standard operating position of the furnace suggests that the joint system is in a static state, forming a frame of two vertical columns and a beam, as shown in **Figure 2**. In this case, the model scheme presents two fixed support points, A and B, determining a system for hyperstatic analysis. However, due to the hinge at point C, the system can be decomposed into two separate subsystems that simplify the formulation.

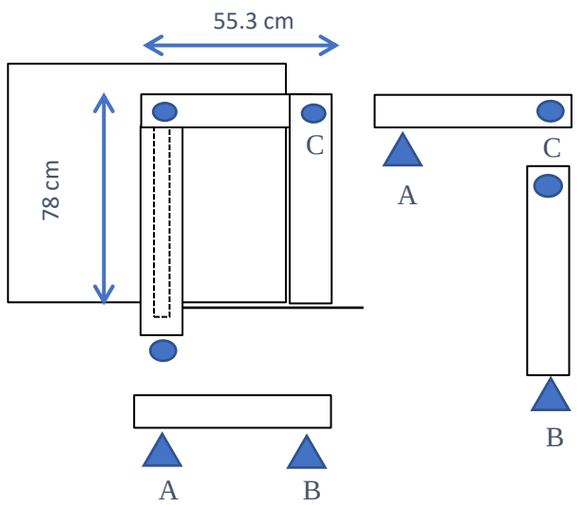

Figure 2 Scheme of the system in a static state for the analysis of reactions proposed with a hyper-static gantry system and as two separate systems due to the existence of the kneecap at point C
Source: Own creation in Microsoft PowerPoint 2016.

ISSN 2523-6776

The system with fixed support at point A must be formulated in the rest condition and during the tilting trajectory. In this way, the schematization of the balance diagrams for both conditions corresponds to the information shown in **Figures 3(a) and 3(b)**, respectively (Nelson, Best, McLean, & Potter, 2010).

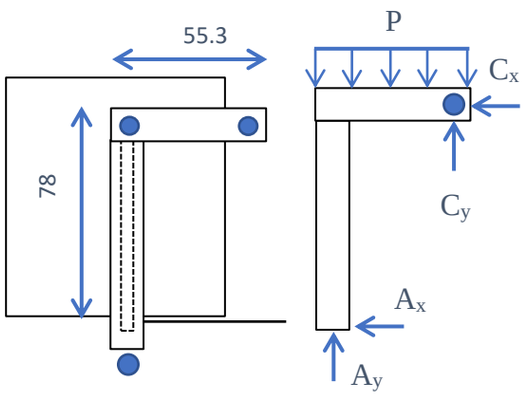

(a)

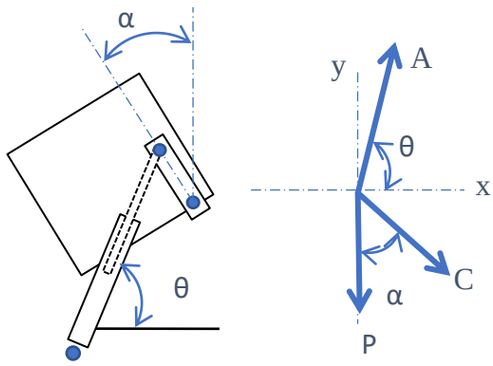

(b)

Figure 3 Diagrams of the system with fixed support at point A under conditions of: a) rest and b) in trajectory during tilting
Source: Own creation in Microsoft PowerPoint 2016.

In the case of the rest position, the balance at point A responds to the reactions A_x and A_y with an effect on C due to the distributed load P. **Equation 1** determines the moment balance about point A.

$$\sum M_A = 0 \rightarrow = \sum M_A\circlearrowright + \sum M_A\circlearrowleft \quad (1)$$

In this way, **Equation 2** results from the analysis of the clockwise and counterclockwise moments of **Figure 3(a)**.

$$\frac{PL}{2} = \frac{PL}{2} + C_x H + C_y L \rightarrow C_y = -C_x \frac{H}{L} \quad (2)$$

In the balance of forces, **Equations 3 and 4** determine the relationship between the components corresponding to points A and C concerning the influence of P.

$$\sum F_{x,A} = 0 \rightarrow A_x = -C_x \quad (3)$$

$$\sum F_{y,A} = 0 \rightarrow A_y + C_y = P \quad (4)$$

Due to the distributed load of P over the section of length L, the system has load symmetry about points A and C. Such that:

$$A_y = C_y = \frac{1}{2}P \quad (5)$$

In this way, calculating the magnitudes of A_x and C_x depends on **Equations 2 and 3**.

$$C_x = -\frac{PL}{2H}; \quad A_x = \frac{PL}{2H} \quad (6)$$

On the other hand, in a trajectory position during tilting, the directions of the resulting forces A and C depend, respectively, on the angles α and θ. Under conditions of instantaneous equilibrium, **Equations 7 and 8** determine the force balance for the scheme in **Figure 3(b)**.

$$\sum F_x = 0 = A\cos(\theta) + C\,sen(\alpha) \quad (7)$$

$$\sum F_y = 0 = A\,sen(\theta) - C\cos(\alpha) - P \quad (8)$$

To know the charge P with the solution of a system of two equations with two unknowns, C is solved for **Equation 7**, defining **Equation 9**.

$$C = -A\frac{\cos(\theta)}{sen(\alpha)} \quad (9)$$

Equation 10 arises by substituting **Equation 9** in **Equation 7** and solving for A, which determines the load experienced at this point, equivalent to the load or force that the cylinder piston overcomes during expansion, that is, in clamping with the furnace.

$$A = \frac{P\,sen(\alpha)}{sen(\theta)sen(\alpha) + \cos(\theta)\cos(\alpha)} \quad (10)$$

ISSN 2523-6776

Calculating the load conditions in each furnace position during tilting depends on **Equations 9, 8, and 3**. Therefore, in the balance of moments about point B, defined by **Equation 11**, the magnitude of the moment is to be counteracted due to the tilting effect.

$$\sum M_B = 0 \rightarrow = \sum M_B\circlearrowright + \sum M_B\circlearrowleft \quad (11)$$

The scheme in **Figure 4** and **Equation 11** establishes that the charges C_y, B_y and C_x are absorbed by the attachment point B and gives rise to **Equation 12**.

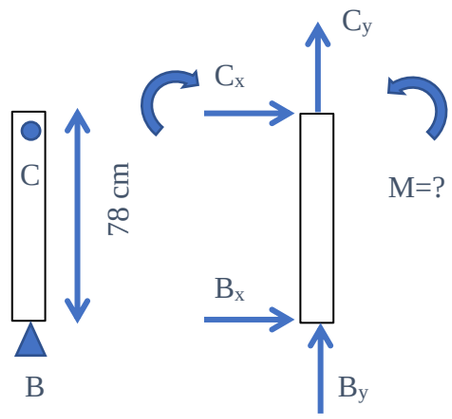

Figure 4 Scheme of reactions in the fixed column with support at point B
Source: Own creation in Microsoft PowerPoint 2016.

$$C_x H = M \quad (12)$$

If a force w existed, keeping the column balanced with the reactions C_x and B_x, **Equation 12**, rewritten as **Equation 13**, indicates that there is a direct proportionality.

$$C_x H = wH\left(\frac{H}{2}\right) \rightarrow C_x = w\left(\frac{H}{2}\right) \quad (13)$$

Obtaining each system component involved in the force balance in the analysis directions depends on **Equations 14 and 15**.

$$\sum F_x = 0 = C_x + B_x \rightarrow C_x = -B_x \quad (14)$$

$$\sum F_y = 0 \rightarrow B_y = C_y \quad (15)$$

On the other hand, the maximum applicable load w depends on the analysis of the profile's resistance capacity used for the column's construction. **Figure 5** shows the internal load diagrams for the conditions of shear force V and bending moment M_f, corresponding to the proposed uniformly distributed load w. The maximum bending moment develops in the shear force plane located at H/2 and is defined by **Equation 16**.

$$M_{fmax} = \frac{1}{4}wH^2 = C_x\frac{H}{2} \quad (16)$$

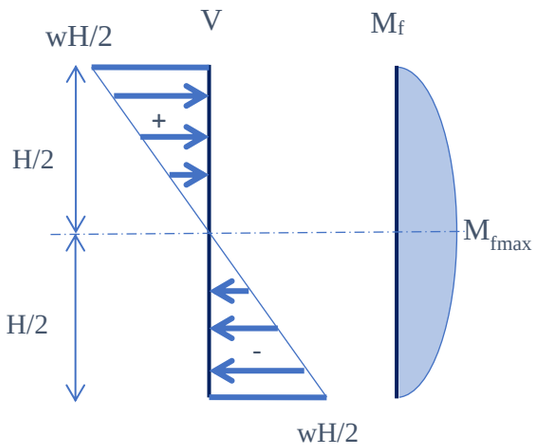

Figure 5 Shear force and bending moment diagrams
Source: Own creation in Microsoft PowerPoint 2016.

While **Equation 17** as defines shear stress:

$$\tau = \frac{VQ}{Ib} \quad (17)$$

Where b is the critical thickness of the profile corresponding to the neutral axis, I represents the moment of inertia, Q is the first-order moment, and V is the maximum shear force, as, for example, for an IPS or IS beam, which has an H-shaped cross-section as shown in **Figure 6**.

ISSN 2523-6776

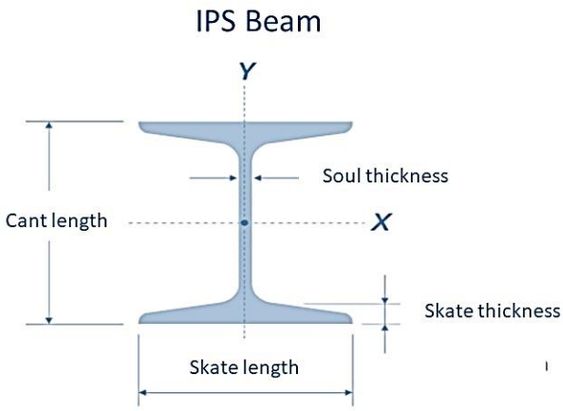

Figure 6 Cross-section drawing of IPS Beam
Source: Image property of (MIPSA, 2023).

Equation 18 allows determining the moment of inertia considering the geometry of the cross-section of the column and the plane on the X-axis (centroid). The corresponding calculation quantifies the cross-sectional surface of the solid shown in **Figure 6**, creating bounded sub-regions in rectangles; the data bf and h represent the length magnitudes of the base and height sides, respectively.

$$I = \frac{b_f h^3}{12} \tag{18}$$

In a similar way, the first-order moment Q is estimated by calculating the sum of the areas of each sub-region bounded by rectangles multiplied by the distance of the centroid of each rectangle to the position of the median plane, considering only the geometric region above the plane concerning the centroid or upper module in the beam.

According to the equilibrium system proposed in **Figure 4**, the magnitude of the shear force V determined through the reaction analysis of the system in **Figure 3(b)** would already be known. Therefore, according to the magnitude of the maximum shear force developed at the support points C and B in **Equation 17**, the maximum shear stress that the material must possess to avoid failure is obtained.

Finally, **Equation 19** defines the stress in the spine due to the bending moment, where c represents the distance from the centroid of the beam to the farthest fiber.

$$\sigma = \frac{Mc}{I} \tag{19}$$

In the case of **Figure 6**, c corresponds to the distance between the position of the X plane and the edge of the beam cant. Therefore, the maximum stress determining the most significant flexion in the spine depends on the ultimate flexor moment.

Results

Equations 20, 21, and 22 determine the displacement trajectories in the articulated element for tilting the furnace schematized in **Figure 7**. Determining the angles α and θ supports the analysis of reactions and determination of forces according to **Figure 3(b)**. **Graphic 1** shows the curves corresponding to these angles as a function of the length of displacement directed by the piston of the hydraulic cylinders.

$$\boldsymbol{a}^2 = \boldsymbol{x}^2 + \boldsymbol{y}^2 \tag{20}$$

$$L^2 = (\boldsymbol{y} - H)^2 + (L - \boldsymbol{x})^2 \tag{21}$$

$$\boldsymbol{y}^2(4L^2 + 4H^2) - \boldsymbol{y}(4H^3 + 4\boldsymbol{a}^2H) + (2\boldsymbol{a}^2H^2 - 4\boldsymbol{a}^2L^2 + H^4 + \boldsymbol{a}^4) = 0 \tag{22}$$

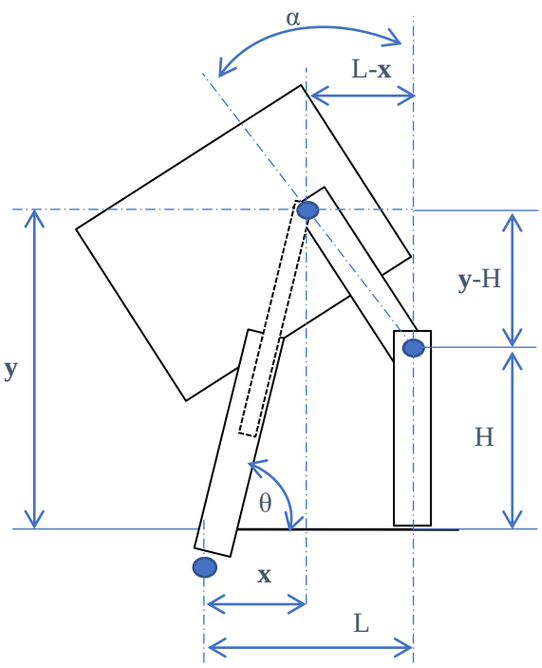

Figure 7 Geometric analysis of the joints for furnace tilting
Source: Own creation in Microsoft PowerPoint 2016

ISSN 2523-6776

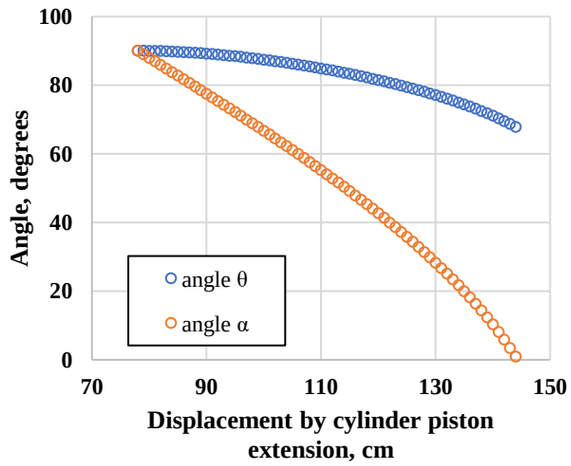

Graphic 1 Curves of the evolution of the angles α and θ defined in the scheme of **Figure 7**
Source: Own creation in Microsoft Excel 2016.

Firstly, determine the magnitude of the force experienced at point A, equivalent to obtaining C according to **Equation 3**. Graphic 2 shows the variation depending on the extension of the cylinder piston and, consequently, the amount of rotation during tilting.

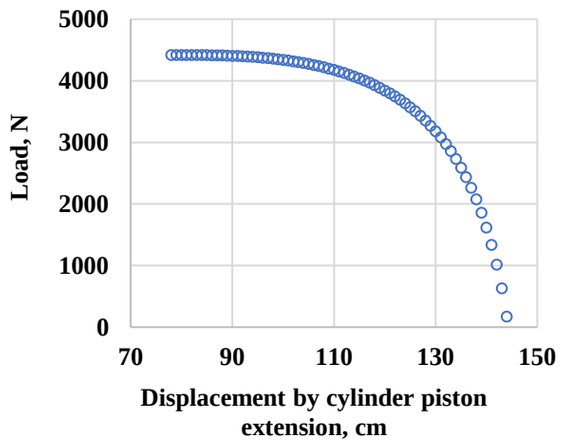

Graphic 2 Curves of the magnitude of the force experienced at point A according to the scheme in **Figure 3(b)**
Source: Own creation in Microsoft Excel 2016.

Interestingly, the force at point A decreases to almost zero once the furnace has reached the fully tilted position logically because the load at that point is a reaction on point B transferred by the column or post. The magnitude of the force experienced at point C corresponds to the sum of the shear and axial forces acting on the column supported at point B, as shown by the curves in **Graphic 3**.

While the axial force is always incremental, the cutting force acquires a maximum (V_{max}) before the full tilt position (α = 25º and θ = 76º) and subsequently decreases to an almost zero condition.

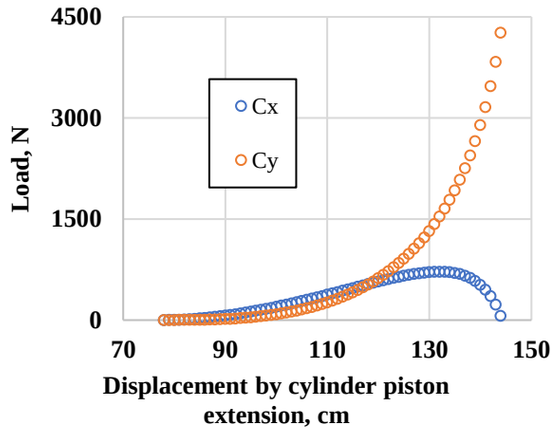

Graphic 3 Curves of the magnitude of the force of the components of the resultant at point C according to the scheme of Fig. 3(b)
Source: Own creation in Microsoft Excel 2016

The magnitudes represented by the curves in **Graphs 2 and 3** correspond to the assumed calculation of a furnace mass in operation of 900 kg. Therefore, according to the load distribution, each system directed on the flanks of the furnace equally supports 4414.5 N. According to this information, **Equations 18 and 19** allow us to obtain the shear stress at point C during the tilting of the furnace and the stress generated in the plane of the maximum bending moment, which is located halfway up the column. (See the curves in **Graph 4**). The calculation of the moment of inertia *I* determined a magnitude of 5070054.48 mm^4, while the first order moment *Q*, with a magnitude of 45795.46 mm^3, considering the following IPS profile specification:

- Cant Length: 127 mm
- Skate Length: 76.3 mm
- Core Thickness: 5.44 mm
- Skate Thickness (average): 8.28 mm
- Location of the centroid plane X: 63.5 mm

ISSN 2523-6776

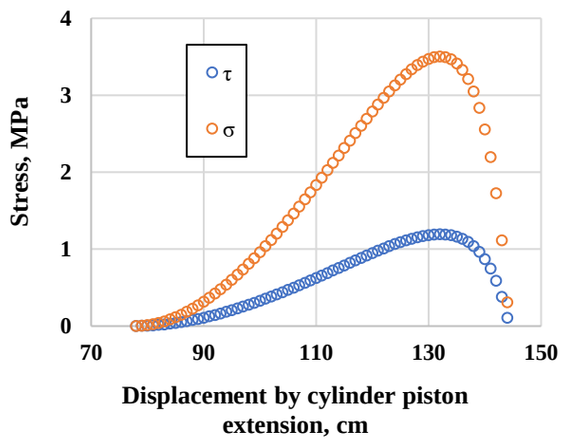

Graphic 4 Curves of the magnitude of shear stress experienced at point C and the stress at mid-height of the column in the plane of development of the bending moment Mf, according to the scheme in **Figure 5**
Source: Own creation in Microsoft Excel 2016.

Regarding the magnitudes of stress, the maximums of both shear and bending coincide with α = 25º and θ = 76º, only considering the shear force C_x. However, there is the axial load associated with the C_y component. The Von Mises criterion provides an equation for determining the static strength criterion and, therefore, the contribution of the compressive load experienced by the column to the maximum shear stress.

In this regard, the calculation of w using **Equation 13** corresponds to the distributed load acting on the column in the direction perpendicular to the compression direction. Such that:

$$w = \frac{2}{H} C_x \tag{23}$$

By definition, the biaxial stress state relates the force C_y through **Equation 24** to the shear stress by principal stresses (Dieter, 1986).

$$\tau_{comp} = \frac{1}{2}\left(\frac{C_y}{S_1} - \frac{w}{S_2}\right) \tag{24}$$

S_1 and S_2 represent the surfaces of the beam where the forces of the main directions act (1: axial, 2: transverse). In this way, the magnitude of w determines the influence of the perpendicular direction (2) on the compression direction (1). However, in this case, it does not modify the generation of shear stress $\tau_{\_comp}$ due to the magnitude of the surface S_2.

Graph 5 presents the curves corresponding to the magnitude of the principal stresses experienced in the column in each furnace position during tilting.

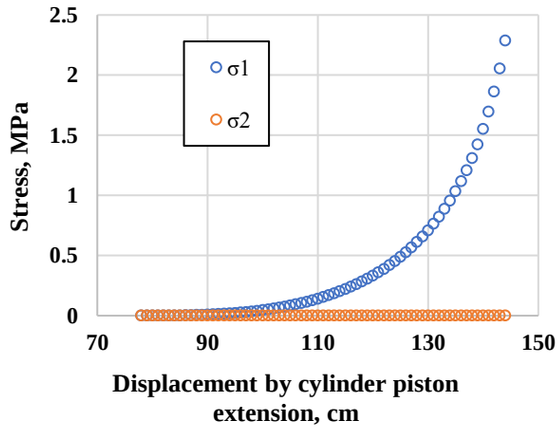

Graphic 5 Curves of the magnitude of principal stresses experienced in the column during the tilting of the furnace
Source: Own creation in Microsoft Excel 2016.

Graphic 6 compares the magnitude of the shear stress in the beam calculated from **Equation 24** with that calculated through **Equation 7**. Note that each case's maximum magnitude of the shear stress is similar. However, in a different tilting condition of the furnace, since, in the case of effect due to principal stresses, the maximum shear stress τ_{comp} is found in the position α = 0.84º and θ = 67.76º or at the end of the total rotation about point C. However, when considering the addition of the shear stresses for the point of maximum influence defined by **Figure 5**, there is a critical interval for α between 25° and 0.84° and for θ between 76° and 67.76°, with the maximum at α = 16.26º and θ = 73.1°.

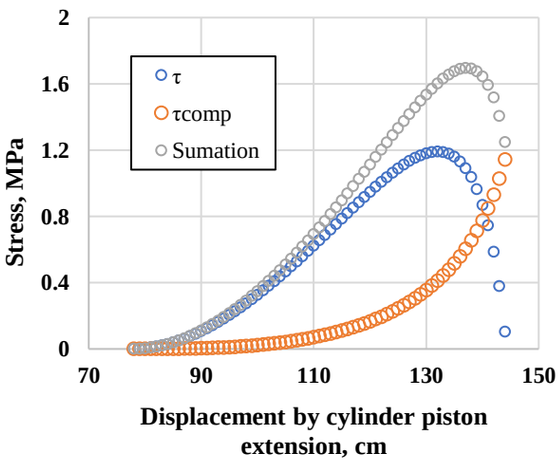

Graphic 6 Curves of the magnitude of shear stresses experienced in the column during the tilting of the furnace
Source: Own creation in Microsoft Excel 2016

ISSN 2523-6776

Defining the Von Mises criterion through **Equation 25** (maximum distortion energy criterion), the magnitude of the estimated stress value due to the effect of the principal stresses determines that the material will not flow if the stress is less than the recorded as the yield of the manufacturing material of the beam that makes up the column; and that in the adopted case corresponds to the IPS structure.

$$\sqrt{\frac{1}{2}((\sigma_1-\sigma_2)^2+(\sigma_1-\sigma_3)^2+(\sigma_2-\sigma_3)^2)} < \sigma_y \quad \textbf{(25)}$$

Since a principal stress acting from a third direction acting from a third direction is not considered, Eq. 25 reduces to the expression of Eq. 26.

$$\sqrt{\frac{1}{2}((\sigma_1-\sigma_2)^2+{\sigma_1}^2+{\sigma_2}^2)} < \sigma_y \quad (26)$$

Graphic 7 shows the result of calculating the effort of the Von Mises criterion. In the curve (empty blue circles), the same behavior shown by the shear stress (τ_{comp}) is identified, although the magnitude is double the amount. Therefore, the maximum state of stress in the column coincides with the position of the furnace in total elevation or at the end of the tilt. Again, the critical interval corresponds for α between 25° and 0.84° and θ between 76° and 67.76°, with the maximum now at α = 18.12º and θ = 73.73° in this case in the position of occurrence of the bending moment.

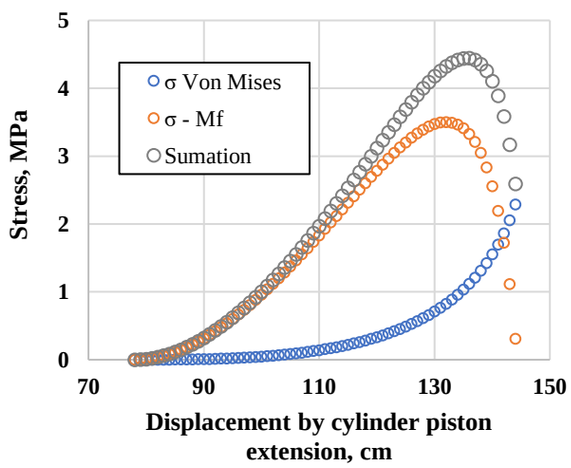

Graphic 7 The magnitude of the Von Mises stress experienced in the column during the tilting of the furnace
Source: Own creation in Microsoft Excel 2016

ISSN 2523-6776

Thanks

The authors would like to thank the Tecnológico Nacional de México, which, through the Instituto Tecnológico de Morelia, provided financial support for the publication of this material.

Conclusions

With the analysis of the stress state strategically planned for the hydraulic cylinder-assisted joint system, the stability of the structures during the operation of high-risk displacement processes is guaranteed. In the example of the furnace with a maximum load of 4414.5 N (450 kg) per flank, a cylinder with a 2-inch diameter piston exceeds the maximum pressure of 248.11 psi since for each unit of power, there would be 3500 psi according to the manufacturer. The material of the IPS beam (ASTM A529 Grade 50) yield stress of 250 MPa would not present deformation during the work sessions.

References

Audet, D., Parent, L., Deveaux, M., & Courtenay, J. (2004). Aluminum Weighing Measurement in Tilting Furnaces. In TMS (Ed.), *Light Metals 2004* (pp. -). Charlotte, North Carolina: The Minerals, Metals & Materials Society.

Dadhania, N., Bhatiya, S., Joshi, A., & Sharma, D. (2016). Review of Cabin Tilting Mechanism for Earth-Moving Machinery. *International Journal Of Advance Research And Innovative Ideas In Education*, 510-514.

Dieter, E. G. (1986). *Mechanical Metallurgy*. McGraw-Hill Series in materials science and engineering.

Hu, J., Pan, J., Dai, B., Chai, X., Sun, Y., & Xu, L. (2022). Development of an Attitude Adjustment Crawler Chassis for Combine Harvester and Experiment of Adaptive Leveling System. *Agronomy, 12*(717), 1-16. doi:https://doi.org/10.3390/agronomy12030717

MIPSA. (2023, Julio 06). *Viga IPS (IS)*. Retrieved from MIPSA Expertos Procesando Metales: https://www.mipsa.com.mx/productos/acero/perfiles-estructurales/viga-ips-is/

Nabertherm. (2023). *Furnaces for Foundry*. Lilienthal, Germany: Nabertherm GmbH. Retrieved from https://www.nabertherm.com/contacts

Nelson, E., Best, C., McLean, W., & Potter, M. (2010). *Schaum's Outline of Engineering Mechanics: Statics*. New York, Chicago, San Francisco, Lisbon, London, Madrid, Mexico City, Milan, New Delhi, San Juan, Seoul, Singapore, Sydney, Toronto: Schaum's McGraw-Hill Companies, Inc.

Sun, H., & Chiu, G. T.-C. (2001). Motion Synchronization for Multi-Cylinder Electro-Hydraulic System. *Proceedings of ASME 2001 International Mechanical Engineering Congress and Exposition* (pp. 1-11). New York: ASME.

Xu, J., & Yoon, H.-S. (2016). A Review on Mechanical and Hydraulic System Modeling. *Journal of Construction Engineering*, 1-11. doi:http://dx.doi.org/10.1155/2016/9409370

ISSN 2523-6776